Separation Science and Technology
Publication details, including instructions for authors and subscription information:
http://www.informaworld.com/smpp/title~content=t713708471

Separation Characteristics of On-chip Biopolymer Membranes

Hisham Mohamed[a]; Anthony P. Russo[a]; Donald H. Szarowski[a]; Elizabeth McDonnell[a]; Lori A. Lepak[b]; Michael G. Spencer[c]; David L. Martin[a]; Michele Caggana[ad]; James N. Turner[ad]
[a] Wadsworth Center, Albany, New York, USA [b] Department of Chemistry and Chemical Biology, Cornell University, Ithaca, New York, USA [c] Department of Electrical and Computer Engineering, Cornell University, Ithaca, New York, USA [d] Department of Biomedical Sciences, The University at Albany, Albany, New York, USA

To cite this Article Mohamed, Hisham , Russo, Anthony P. , Szarowski, Donald H. , McDonnell, Elizabeth , Lepak, Lori A. , Spencer, Michael G. , Martin, David L. , Caggana, Michele and Turner, James N.(2007) 'Separation Characteristics of On-chip Biopolymer Membranes', Separation Science and Technology, 42: 1, 25 — 41
To link to this Article: DOI: 10.1080/01496390601057973
URL: http://dx.doi.org/10.1080/01496390601057973

Separation Science and Technology, 42: 25–41, 2007

ISSN 0149-6395 print/1520-5754 online
DOI: 10.1080/01496390601057973

Separation Characteristics of On-chip Biopolymer Membranes

Hisham Mohamed, Anthony P. Russo, Donald H. Szarowski, and Elizabeth McDonnell
Wadsworth Center, Albany, New York, USA

Lori A. Lepak
Department of Chemistry and Chemical Biology, Cornell University, Ithaca, New York, USA

Michael G. Spencer
Department of Electrical and Computer Engineering, Cornell University, Ithaca, New York, USA

David L. Martin, Michele Caggana, and James N. Turner
Wadsworth Center, Albany, New York, USA and Department of Biomedical Sciences, The University at Albany, Albany, New York, USA

Abstract: Research in miniaturization of microfluidic devices and total analysis systems for chemical and biological applications has been active for more than a decade. Sample size and processing time have decreased dramatically, while sensitivity has increased, along with the ability to run multiple tests in parallel. However, sensitivity depends in most cases on the purification or enrichment of the sample prior to loading onto a device. Filtration is performed either prior to sample loading or through membranes adhered to the substrate. Currently, these membranes cannot be patterned to micrometer resolution and the adhesion process may be incompatible with the fabrication and/or may introduce contaminants to the process.

Received 7 March 2006, Accepted 29 August 2006
Address correspondence to James N. Turner, Wadsworth Center, and Department of Biomedical Sciences, The University of Albany, New York 12201-0509, USA. E-mail: turner@wadsworth.org

We have developed a process to incorporate filtration onto microfluidic devices that is compatible with microfabrication methods and is suitable for biological applications. We cast cellulose acetate membranes directly onto silicon wafers without the use of adhesives and studied the filtration properties of these membranes using compounds with molecular weights ranging from 100 to 900. We also have varied the casting conditions and studied the effects of these variations on the membrane's rejection characteristics. Cellulose acetate membranes, cast directly onto silicon wafers, adhered well to the substrate and had high structural integrity. We have developed membranes with four different molecular weight cut-offs; 300, 350, 600, and 700Da. Parameters such as solubility and charge were also investigated for their contribution to the rejection characteristics.

Keywords: Lab-on-a-chip, cellulose acetate, filtration, on-chip molecular separation

INTRODUCTION

The miniaturization of analytical systems has been motivated by the need to enhance analytical performance, decrease reagent consumption, reduce test time, provide the potential of running multiple tests in parallel, and integrate multiple functions, such as sample handling, analysis, and detection, into a single device (1, 2). This field has evolved rapidly since its debut around 1975 by adapting microfabrication techniques from the semiconductor industry to what is now called micro total analysis systems or lab-on-a-chip.

An integrated on-chip system is capable of controlling fluid transport, separations, purification, sensing and/or detection (3). Systems have been developed for specific biological applications such as protein separations, polymerase chain reaction (PCR), DNA separation and sequencing, and clinical diagnostics (4, 5).

In many systems, sample purification or pre-concentration is required to enhance the device's sensitivity and specificity and these strategies have focused mainly on chromatographic or electrophoretic separation (6–8). While these methods have enabled the use of highly sensitive detectors that are capable of quantifying extremely low concentrations of uncontaminated solute, they have not been adequate for separating highly complex mixtures, such as a biological fluid. Membrane separation may be an efficient method for simple size (sieving) and/or electrostatic separations in the lab-on-a-chip environment (9). Previously, filtration has been either performed prior to sample loading or through the use of pre-formed membranes adhered to the substrate (10, 11). However, these membranes cannot be patterned with the fine resolution required for microfabricated devices. Furthermore, the adhesion may be incompatible with fabrication processes, and/or may introduce contaminants from adhesives or filter dust (10, 12). While some groups have incorporated the membranes into chip-based devices for cell-culture application, others have etched small pores into the silicon substrate itself (13–16). The latter method provided precise control of pore

size, but at the expense of fabrication time and cost. Filtration has also been achieved through manipulation of microfluidics, by using multiphase flow as a liquid membrane or by creating polymer membranes using interfacial polymerization within the microchannels (17). In some cases, pore sizes smaller than 200 nm were reported. However, a possible drawback to these methods is the limited surface area available for mass transfer (18).

Our group's main objectives are to integrate filtration onto microfluidic devices in a way that is compatible with existing microfabrication processes, and to develop a methodology for changing the membrane's chemistry and rejection characteristics, to render it suitable for a wide range of biological applications. We are investigating the use of polymer membranes, and this paper presents results obtained using cellulose acetate.

In previous work, we have demonstrated the ability to cast the membranes directly on silicon wafers and to form pores using the wet inversion process without adhesives, resulting in good adhesion to the substrate and structural integrity. The casting of the membranes on an etched silicon wafer with the additional microfluidics cast in PDMS provided a fully functional, on-chip separation system (19, 20). In this paper, we extend this work by identifying the process parameters and manipulating them to alter the molecular weight cut-off (MWCO) to create a range of membranes for different applications.

Additionally, we examined the membrane rejection characteristics by studying other factors that contribute to the molecular rejection of the membrane, such as charge and solubility.

METHODS

The fabrication process, similar to the one described by Russo and coworkers 2004, can be summarized as follows: single side polished 3″ silicon wafers were cleaned and coated on both sides with 200 nm of low-stress silicon nitride using low-pressure chemical vapor deposition (19, 20). A two-dimensional array of squares ranging from 2 μm by 2 μm to 8 μm by 8 μm was patterned in the silicon nitride on the top side of the wafer (polished side) by using standard photolithography techniques, and the silicon nitride layer was etched using reactive ion etching. The process was repeated on the backside (unpolished side) using a second mask containing arrays of 1 mm by 1 mm squares aligned with the previously patterned regions on the polished side. After the silicon nitride was patterned on the backside by reactive ion etching, the interstitial layer of silicon was removed by etching in potassium hydroxide (KOH) (40% v/v) solution at 90°C. The remaining silicon nitride on the unpolished side was the masking material for the KOH etch step to limit the KOH etch to the 1 mm^2 windows. The resulting substrate consisted of a silicon wafer with a 200 nm silicon nitride layer suspended across 1 mm^2 holes etched completely through the wafer as shown in Fig. 1 (steps 1 to 3). This suspended layer has the array of 2 μm

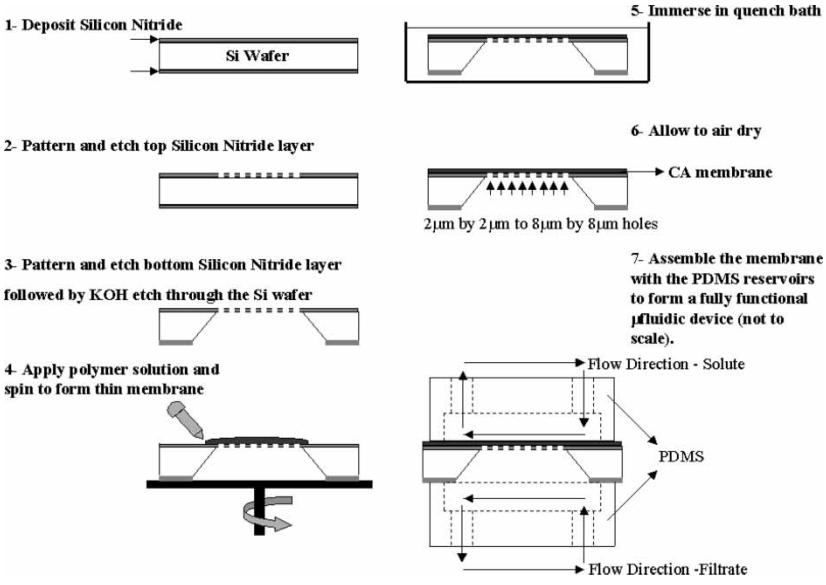

Figure 1. Summary of the fabrication process.

by 2 μm to 8 μm by 8 μm square holes. Following the KOH etch, the silicon wafers were rinsed with deionized water, isopropyl alcohol, and allowed to air 2dry.

Membranes were cast directly onto the silicon wafers from cellulose acetate (CA) solutions by spinning the polymer solution onto the wafers. A blank wafer was attached to the spinner with a vacuum chuck and the etched wafer adhered to the blank wafer with double – sided tape. The wafer was cleaned with isopropyl alcohol, and primed with P20 (purchased from Shipley, Marlborough, MA) solution to promote membrane adhesion. P20 is a 20% hexamethyldisilazane and 80% propylene glycol monomethyl-ether acetate based product used to promote adhesion on silicon wafers. Polymer solutions were prepared by dissolving CA (39.8 wt% acetyl content, $M_w = 30{,}000$), in N,N−dimethylacetamide (DMAc), both purchased from Sigma Aldrich (St. Louis, MO), at various concentrations, as described in the RESULTS section below. Spinning times and speeds varied from 5 to 30 sec and 2000 to 3000 rpm. After spinning, the coated wafers were immersed in a water bath for 10 min at various controlled temperatures, removed and allowed to air-dry as shown in Fig. 1 (steps 4 to 6). The thickness of membranes spun from 25% CA in DMAc (w/v) solution ranged from 25 μm to 120 μm, as measured with a high-accuracy length gauge (MT12, Heidenhain Corp., Schaumburg, IL), and/or scanning electron microscopy (SEM).

For flow experiments, the membrane was attached to two reservoirs with inlet and outlet channels, one reservoir on each side of the membrane.

Fluid reservoirs were molded from a silicon wafer patterned using SU8 photoresist (Micro Chem Newton, MA). To make the SU8 master, a blank wafer was cleaned with acetone, isopropyl alcohol, rinsed with deionized water, dried with nitrogen, and placed on a hot plate at 200°C for 5 min. Two layers of SU8 were applied to the wafer to achieve the total thickness of 85–90 μm. Each layer was first spun at 500 rpm for 10 sec, then at 1000 rpm for 30 sec, both times with slow acceleration (5 sec). The coated wafer was then soft baked on a hot plate at 65°C for 1 min then at 95°C for an additional 3.5 min. The second layer was applied using the same conditions with the exception of increasing the bake time at 95°C to 11 min. The wafer with both SU8 layers was exposed for 11 min (UV lamp was 400–450 $\mu W/cm^2$) and developed for 3–5 min in SU8 developer (Micro Chem, Newton, MA), rinsed in isopropyl alcohol, dried with nitrogen, and hard baked on a hot plate at 200°C for 5 min. The photoresist at this point was fully cured, and was used as a master to mold the reservoirs in polydimethylsiloxane (PDMS) for the flow experiments. To prepare the reservoirs, the two components of the PDMS (GE RTV615, General Electric, Pittsfield, MA) were mixed in a 10:1 ratio (w/w), degassed for 15–30 min to remove any dissolved air, poured into the mold and degassed a second time to perfectly mold to any small feature on the SU8-coated wafer. Next, the PDMS was cured at 60°C for one hr. After curing, the PDMS was removed from the mold, tubing ports were punched into the reservoir area, and silicone tubing was inserted. The PDMS was cleaned with a laboratory glass cleaner, rinsed with deionized water, isopropyl alcohol, and dried with nitrogen. The PDMS was cleaned in O_2 plasma for 3 minutes using a Harrick PDC-001 Plasma Cleaner (Ossining, NY). Upon removal from the plasma cleaner, the reservoir was aligned and pressed onto the membrane-coated wafer, creating a fluid seal (Fig. 1, step 7). The reservoir on each side was connected to a Brinkmann IP4 peristaltic pump (Ismatech, Zurich, Switzerland), which circulated the feed and filtrate solutions.

To test the transport across the membrane, 4–5 mM aqueous solutions of the test compounds were pumped tangentially to the membrane surface for 90 min, while deionized water was pumped tangential to the other side, each at 200 μL per minute (all molecular weights of all compounds are listed in Table 1 and were purchased from Sigma Aldrich, St. Louis, MO). The absorbance of the filtrate was measured with a Beckman DU600 spectrophotometer and the concentration calculated using the appropriate molar extinction coefficient.

For the experiment measuring molecular binding to the membranes, described under RESULTS, we used the Corning Transwell® Inserts, (Corning, Acton, MA) as a frit to spin the CA membrane onto instead of ontosilicon wafers. Membranes were cast using the same procedure as on the wafers. Inserts were removed from the wells and turned over, taped to a blank wafer, and the polymer solution was spun on top. Both types of membrane used in this experiment were made using 25% CA in DMAc,

Table 1. Summary of compounds used

#	Molecule	MW	
01	Sodium nitrate	84.99	
02	L-Tyrosine	181.19	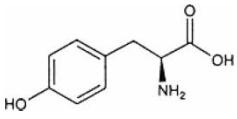
03	Caffeine	194.12	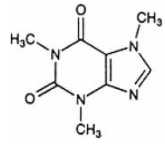
04	L-Tryptophan	204.23	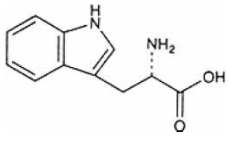
05	Methyl-red	269.30	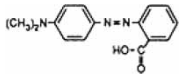
06	Toluidine-Blue-O	305.83	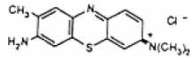
07	Methyl orange	327.34	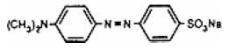
08	Phenol-red	354.38	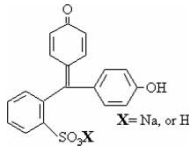
09	Ethyl violet	492.15	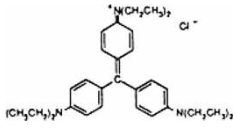
10	Alizarin blue-black (Mordant black 13)	610.62	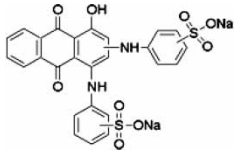
11	Congo red	696.67	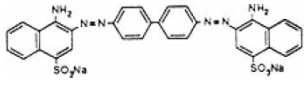

spun at 2000 rpm for 5 sec, and quenched in water for 10 min. One set (n = 3) of membranes was quenched at room temperature and the second set (n = 3) was quenched at 35°C. These were the same conditions that had been used for spinning membranes on the silicon wafers. Several experiments were performed to ensure that spun membranes on inserts had the same MWCO as membranes spun on silicon wafers (results not shown).

A Bio-Rad MRC600 confocal system mounted on an Olympus IX-70 inverted microscope using a 40 × (1.15 NA)-objective lens was used for confocal scanning laser microscopy. The fluorescent molecule was excited at 488 nm. The images, 25 optical slices spaced at 1 μm in the z-dimension, were collected as a three-dimensional stack and presented as a maximum intensity value projection using BIO-RAD™ and ANALYZE™ software.

RESULTS

The variation in molecular flux across the membrane for molecules ranging from 62Da (nitrate) to 354Da (phenol red) was reported previously (20). This membrane was cast from a solution of 25% CA (Type II in Fig. 2) dissolved in DMAc (w/v), spun at 2000 rpm for 20 sec and quenched in a water bath at room temperature for 10 min. The transmembrane fluxes of the solutes decreased with increasing MW, with nitrate ions having the highest flux and almost no trace of phenol red flux (20).

Solvents, mixing concentrations, casting conditions such as spin parameters, quenching solutions and temperatures, and potentially post-processing and treatment are expected to affect in some respect the membrane's rejection characteristics. For this study, we only used CA and

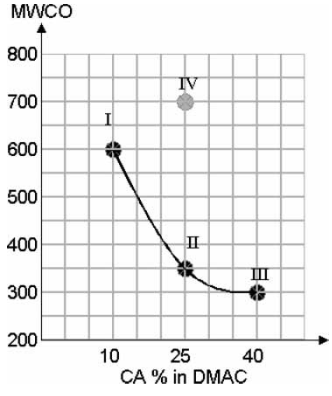

Figure 2. Shows control of the molecular weight cut-off (MWCO) for four different membranes with different casting conditions: (I) 10% CA in DMAc, (II) 25% CA in DMAc quenched at room temperature, (III) 40% CA in DMAc, and (IV) 25% CA in DMAc quenched at 35°C.

we investigated the effects of its concentration in DMAc, quenching bath temperatures in deionized water, and spin speed and time on the rejection characteristics. Changes in polymer concentration were expected to affect the pore sizes and thus the rejection characteristics. For confirmation of this, additional membranes were cast from 10% (Type I in Fig. 2) and 40% (Type III) CA, both preparations used DMAc (w/v), were spun at 2000 rpm for 30 sec, and quenched in water for 10 min at room temperature. The membranes cast from 10% CA excluded 600 Da molecules (Alizarin Blue Black, MW 610, Table 1), and membranes cast from 40% CA excluded 300 Da molecules (ethyl red, MW 297). However, the 40% CA solution was viscous and resulted in a thick membrane that was often uneven and had air bubbles, decreasing the yield. Additionally, the surface of the membrane became wrinkled when dried, often making them unusable. To alleviate this problem, we kept the membranes wet at all times after the quenching step making it more difficult to assemble them into devices.

Experimentation with the quench bath temperature revealed alterations in pore formation and membrane transport characteristics. Membranes made of 25% CA dissolved in DMAc and spun at 2000 rpm for 5 sec, and quenched in deionized water for 10 min at 35°C (Type IV) were tested for filtration characteristics. These membranes passed phenol red, rejected previously by similar membranes quenched at room temperature, but they rejected Congo red, which has a MW of 696. MWCO results are summarized in (Fig. 2, Table 2).

Both, the speed and duration of spinning affected the membrane thickness (20). To examine the difference in filtration properties, we compared two membranes made of 25% CA dissolved in DMAc and spun at 2000 rpm for either 5 or 20 sec, and quenched in deionized water for 10 min at room temperature, using caffeine, and phenol red. Both membranes rejected phenol red, as expected, and passed caffeine, although at different rates; the thinner membrane (approximately 30 μm) passed the caffeine almost 1.5 times faster than the thicker membrane (approximately 40 μm) (Fig. 3).

To further characterize the membranes, we studied the binding of positively charged molecules to the membrane. For this study, we spun the membranes onto Transwell® inserts, as shown in Fig. 4, in order to increase the area of transport and, thus, better quantify the amount of bound material. After casting the membranes onto the inserts but prior to running the experiments, we immersed the inserts in deionized water and let them degas for five minutes to ensure that they were completely wetted. Then one mL of aqueous solution of the test compounds was placed in the top compartment and one mL of water was placed in the bottom compartment. The inserts were left for 6 hr to allow the molecules to diffuse through the membrane. Next, the absorbance of the feed and the filtrate were measured, and compared to the value of the original solution prior to loading. All solutions were in the linear range of absorbance versus concentration. Therefore, the ratio of the absorbances is equal to the ratio of the concentrations, which since the volumes were equal and constant corresponds to

Table 2. Summary of MWCO results

Membrane	Casting conditions	MWCO[a] (Da)	Notes
Type I	10% CA in DMAc (w/v), spun at 2000 rpm for 5 sec, quenched in water at room temperature for 10 min	600	Decrease in polymer concentration (from our standard process membrane Type II) lead to a higher MWCO
Type II	25% CA in DMAc (w/v), spun at 2000 rpm for 5 sec, quenched in water at room temperature for 10 min	350	Our standard process for casting membranes, changes in spinning speed or time had an effect on the thickness and thus the rate at which molecules passed, but not the MWCO
Type III	40% CA in DMAc (w/v), spun at 2000 rpm for 30 sec, quenched in water at room temperature for 10 min	300	Increase in polymer concentration lead to a lower MWCO, but the membranes had more stresses limiting their use.
Type IV	25% CA in DMAc (w/v), spun at 2000 rpm for 5 sec, quenched in water at 35°C for 10 min	700	Increase in quenching bath temperature lead to increase in MWCO

[a]MWCO is defined as the MW of a solute at which 95% separation can be achieved.

the ratio of the amount of each molecule. If the test compound did not bind to the membrane, the sum of the absorbance in the two compartments will be equal that of the original solution. The amount absorbed onto the membrane was obtained from the difference between the sum of the absorbance on both sides of the membrane and the absorbance of the original solution. Four molecules were used individually to test membranes quenched at room temperature (MWCO = 350): caffeine, L-tryptophan, toluidine blue O, and methyl orange. Our results showed that the membrane absorbed up to six times more toluidine blue O than any other compound tested (negative results indicates at or below the detection limits) (Fig. 5a). Similarly, we tested the membranes quenched at 35°C with ethyl violet, phenol red sodium salt, and congo red. The positively charged molecule (ethyl violet) was significantly bound to the membrane (Fig. 5b). The membranes were, in fact, visibly stained by toluidine blue O and ethyl violet and the color was not removed when the membranes were soaked in deionized water for up to 24 h.

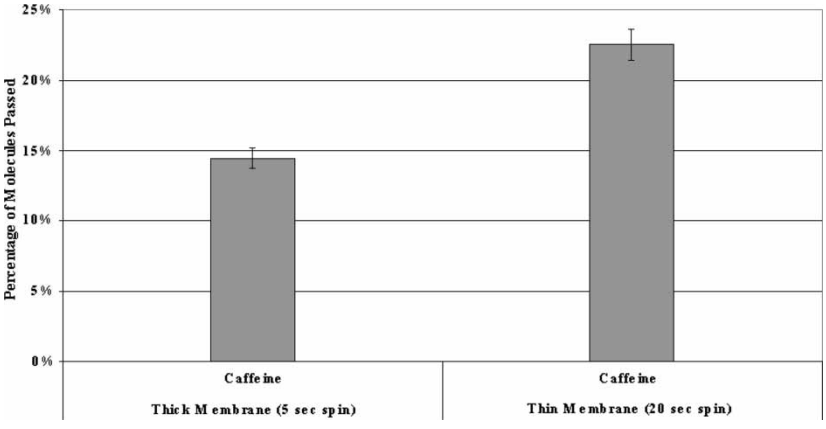

Figure 3. Comparison of the percentage of molecules that passed across two membranes with different thickness, the thinner membrane (approximately 30 μm) transported caffeine approximately 1.5 times faster than the thicker one (approximately 40 μm).

When these membranes were imaged using SEM, we observed a thin skin, 20 to 30 nm thick, and large voids, up to several micrometers in width and depth, in the interior. No visible pores were found on the skin surface using SEM. To test the contribution of the voids on filtration, a solution containing a fluorescent molecule, which was smaller than the MWCO (3,6-diaminoacridine hemisulfate- proflavine, MW 258 Da), was added on one side of the membrane and left overnight in the dark to diffuse through. The dye distribution in the membrane was imaged while the membrane remained immersed in the dye solution by confocal laser scanning microscopy. We observed fluorescence through the whole membrane except for the areas where there were large voids, suggesting that molecules did not penetrate into the voids. An optical section in focus in the middle of the membrane is shown in Fig. 6, and shows that the fluorescent dye is absent from inside the voids while the surrounding matrix fluoresced brightly. Additionally, when membranes were treated chemically, leading to changes

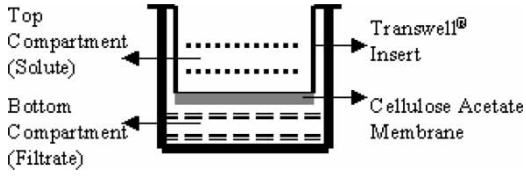

Figure 4. Schematic of the commercial Transwell® inserts showing the top and bottom compartments for the feed and filtrate respectively, separated by the CA membrane which was supported by the polycarbonate Transwell® membrane that had 0.2 micrometer pores.

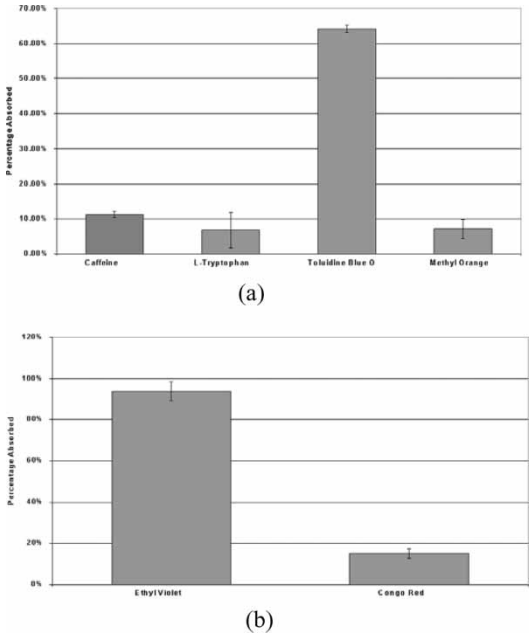

Figure 5. (a) Comparison of absorption of four different molecules in the membrane with 350 Da MWCO (25% CA in DMAc, quenched at room temperature) showing that only the positively charged molecule, Toluidine Blue O, binds significantly. (b) Similarly, ethyl violet (positively charged) binds significantly to the membrane with 700 Da MWCO (quenched at 35°C) compared to Congo Red.

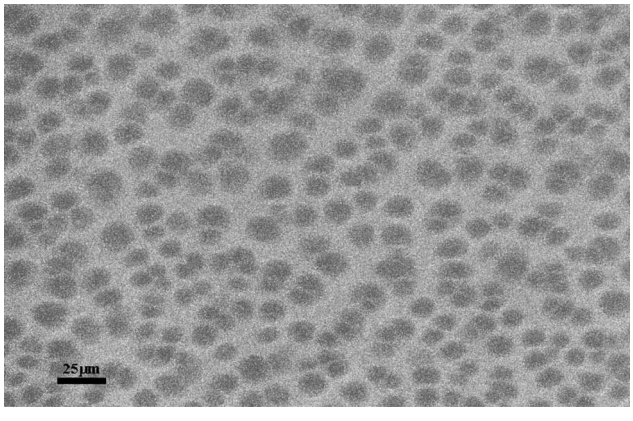

Figure 6. Image of the stained membrane collected by confocal laser scanning microscopy showing fluorescence across the whole membrane except for the areas of the large voids. This is one in-focus X-Y slice in the middle of the membrane out of the 25 slices collected along the Z-axis. The dark areas have no fluorescence and correspond to the voids.

in void characteristics, ranging from the absence of voids to the presence of large voids spanning approximately across the whole membrane thickness but not penetrating the surface skin, there was no change in the MWCO for the compounds tested (Fig. 7). The membrane treatment consisted of incorporating carboxymethylcellulose (CMC) (Sigma Aldrich, St. Louis, MO) in the quenching bath. An initial quench of the 25% CA in DMAc membrane in 1% CMC in deionized water followed by a second quench in deionized water, resulted in large voids that extended through the membrane thickness but did not penetrate the surface skin of the membrane. An initial quench of the 25% CA membrane in DMAc in 1% CMC in 30% Acetic Acid followed by a second quench in deionized water did not produce large voids in the membrane interior. Generally, large voids are undesirable since they affect the membrane's structural integrity (21).

DISCUSSION AND CONCLUSIONS

Membranes made of 10% and 25% cellulose acetate dissolved in DMAc were cast successfully onto silicon wafers and the polycarbonate membrane of Transwell® inserts showed structural integrity and good adhesion to the substrate. However, membranes cast from a 40% CA solution were less reproducible due to increased viscosity resulting in occasional non-uniform coatings, and to high stresses in dried membranes. Thus, these membranes were kept wet at all times limiting their practicality in an assembled microfluidics device. Additional research will focus on decreasing the MWCO by use of different polymers and/or solvents, and different casting and quenching conditions.

Membrane binding experiments showed that negative and neutral molecules, with molecular weights smaller than the MWCO passed without significant binding to the membrane. However, positively charged molecules were bound to the membrane. A possible explanation is that CA contains many partially negatively charged, sterically accessible oxygen atoms that can interact with the positively charged solutes in a similar fashion to solvation. In contrast the partially positive carbon atoms to which the oxygens are attached are much less sterically accessible than the oxygens. Thus, negatively charged molecules cannot interact well with them and do not bind to the membrane. The cation interactions may be similar to those known to occur with oxygen rings in crown ethers (22). This would explain why positive molecules were retained while negative molecules were not rejected since the rest of the cellulose acetate molecule would still be neutral with the partial negative charge localized. Incorporation of compounds such as crown ethers into membranes will be investigated in the future to selectively retain molecules of interest. We will also study the binding mechanism, which is necessary to further manipulate the pore sizes. Incorporation of specific functional groups onto the surfaces of the membranes will also be investigated in order to selectively retain molecules of interest.

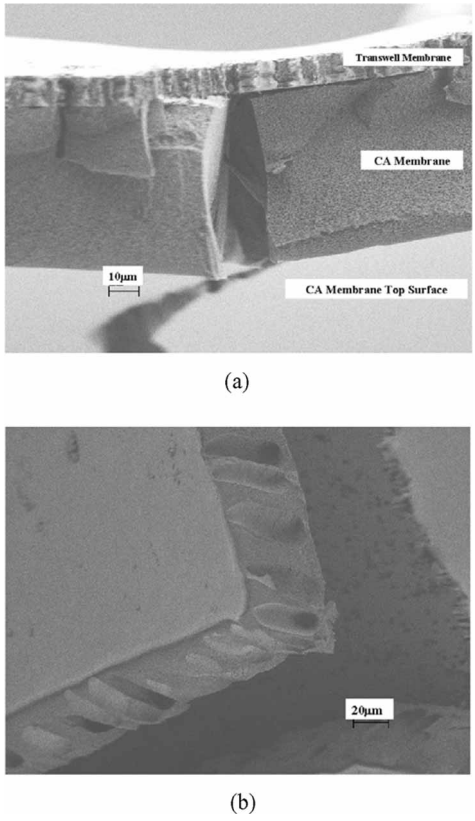

Figure 7. SEM of fractured membranes showing the internal structure of the CA membrane without internal voids when quenched in a carboxymethylcellulose solution (a), and with voids when the membrane was quenched in pure water (b). Figure in (b) also clearly shows the surface skin.

Flux across the membrane tended to increase as the molecular weight and molecular size decreased but there was sufficient variation, including the fact that some larger molecules crossed the membrane more readily than smaller ones, therefore no statistical inferences could be drawn. For example, the flux of the toluidine blue O (MW 305Da) was an order of magnitude greater than that of methyl red (MW 269) despite it having a larger MW (Fig. 8). Similarly, tryptophan (MW 204Da) and caffeine (MW 196Da) had a higher flux than tyrosine (MW 181 Da). Interestingly, in each of these examples the solubility of the larger molecule was greater than the solubility of the smaller molecule. Solubility of the molecules in water (23, 24) did not provide a consistent explanation of the flux data. The flux of the higher molecular weight organic molecules did not show a dependence on solubility, while there may be a trend for the lower molecular weight organic

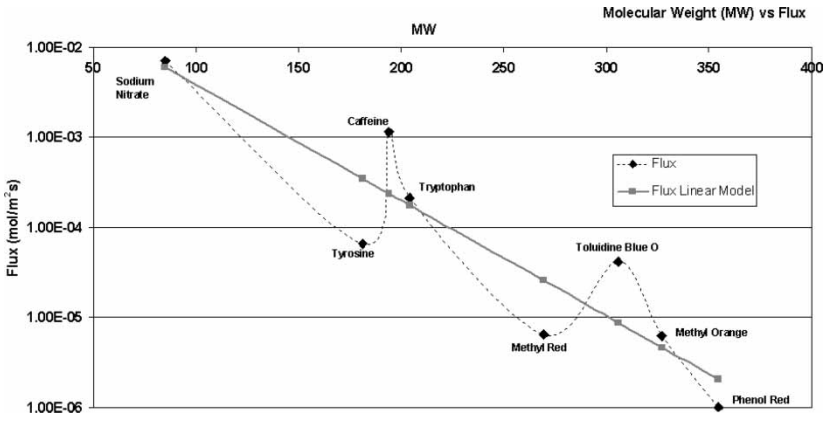

Figure 8. Plot for MW versus measured flux and the linear fit of the measured flux showing a decrease in flux with increase in molecular weight.

molecules (25). It is not a strong trend and the relationship is complex. It is difficult to understand the influence of solubility, since at the molecular level solubility is a very complex phenomenon driven by the free energy difference between the solid state and the dissolved state. The dissolved state is influenced by charge-dipole or dipole-dipole interactions among individual molecules of solvent and solute, and in our case, between the solute and the surfaces of the membrane. Any solvent-solute interaction replaces a solvent-solvent or solute-solute interaction or the interaction of the solvent or solute with the membrane with a consequent change in the free energy of the system. The stronger the solvent-solute interaction, the relatively weaker the membrane-solute interaction will be, with some consequences for the bulk transport of the solute; this is the molecular basis, for example, for most forms of chromatography and may help to explain our observations. However, the fluxes of these molecules are clearly dependent on a number of factors and not dominated by a single factor. Charge and relative electron negativity are also important parameters.

Experiments using fluorescent molecules suggest that the voids in the interior of the membranes have no role in the filtration mechanism. Confocal microscopy demonstrated that the voids contained no fluorescence even after soaking the membranes with a fluorescent molecule that readily passed through the membrane. The matrix surrounding the voids was strongly fluorescent indicating that the molecules readily filled the matrix but did not fill the voids. This combined with the fact that the filtration results were similar and independent of the presence of the voids suggests that the membranes were composed of a matrix that defined the transport properties of the membrane and voids that were isolated from the matrix.

Altering the casting conditions lead to differences in MWCOs and molecular fluxes. Starting from the 350 Da size rejection, we effectively increased and decreased the MWCO to a range of 300Da and to 700Da respectively. Increasing polymer concentration in the solvent decreased the effective pore size and decreased the MWCO while increasing the quenching bath temperature increased the effective pore size and the MWCO. Identification of parameters that control the rejection characteristics is a major step towards achieving a family of on-chip membranes with different rejection characteristics for various biological applications. When membranes were made with different thickness, the molecular flux increased for thinner membranes but the MWCO remained the same, i.e the flux and MWCO are independent.

Integration of filtration within microfluidic devices is a major step toward achieving complete functionality on-chip. This utility can be a front-end or an intermediate step applicable to many analysis devices. Ultimately, their incorporation will result in an enriched, more purified sample from a complex input mixture leading to more sensitive detection.

The main objectives of this project were to integrate filtration into a microfluidic device in a compatible way using existing microfabrication processes, and to develop a methodology of altering the membrane's chemistry and rejection characteristics to be suitable for biological applications. Thus, the experiments were not designed to test for every condition and every process, but to define the main parameters governing the rejection and surface characteristics and how to modify the membrane for a certain application. Our group has successfully used the type II membrane (MWCO 350 Da) to purify DNA from heme prior to running PCR (polymerase chain reaction) to amplify the DNA. Single stranded DNA was driven electrophoretically through the membrane while the heme (MW 614) was blocked (27). This has important implications because heme inhibits PCR, co-migrates with DNA under conventional electrophoretic conditions, and is present at high concentrations in DNA prepared from dried blood spots. This method is also not reaction specific, which is an advantage over existing methods that reduce the influence of small molecules that inhibit PCR (26, 27). Additionally, these membranes can be used for cell co-culture studies, where control over the exchange of the signaling molecules is valuable to investigate a specific cellular response. Both these applications are currently being pursued.

ACKNOWLEDGMENT

This work is supported by the STC Program of the National Science Foundation under Agreement No. ECS-9876771. The authors acknowledge the assistance of the Biochemistry Core and the Electron Microscopy Core at

the Wadsworth Center, which is supported in part by the National Science Foundation Grant DBI-0116551. This work was performed in part at the Cornell Nanofabrication Facility (a member of the Nanotechnology Infrastructure Network) which is supported by the National Science Foundation under Grant ECS-9731293, its users, Cornell University and Industrial Affiliates.

REFERENCES

1. Reyes, D.R., Iossifidis, D., Auroux, P.A., and Manz, A. (2002) Micro total analysis systems. 1.1 introduction, theory, and technology. *Anal. Chem*, 74: 2623–2636.
2. Kutter, J.P. (2000) Current developments in electrophoretic and chromatographic separation methods on microfabricated devices. *Trends Anal. Chem.*, 19 (6): 352–363.
3. Broyles, B.S., Jacobson, S.C., and Ramsey, J.M. (2003) Sample filtration, concentration, and separation integrated on microfluidic devices. *Anal. Chem.*, 75: 2761–2767.
4. Yu, C., Davey, M.H., Svec, F., and Frechet, J.M.J. (2001) Monolithic porous polymer for on-chip solid-phase extraction and preconcentration prepared by photoinitiated in situ polymerization within a microfluidic device. *Anal. Chem.*, 73: 5088–5096.
5. Xu, Y. and Bao, G. (2002) A filtration-based protein microarray technique. *Anal. Chem.*, 75: 5345–5351.
6. Bruin, G.J. (2000) Recent developments in electrokinetically driven analysis on microfabricated devices. *Electrophoresis*, 21: 3931–3951.
7. Rossier, J., Reymond, F., and Michel, P.E. (2002) Polymer microfluidic chips for electrochemical and biochemical analyses. *Electrophoresis*, 23: 858–867.
8. Auroux, P.A., Iossifidis, D., Reyes, D.R., and Manz, A. (2004) Micro total analysis systems. 2. Analytical standard operations and applications. *Anal. Chem.*, 74: 2637–2652.
9. Ismail, A.F. and Hassan, A.R. (2004) The deduction of fine structural details of asymmetric nanofiltration membranes using theoretical models. *Journal of Membrane Science*, 231: 25–36.
10. Wang, P.-C., DeVoe, D.L., and Lee, C.S. (2001) Integration of polymeric membranes with microfluidic networks for bioanalytical applications. *Electrophoresis*, 22: 3857–3867.
11. Wang, P.-C., Gao, J., and Lee, C.S. (2002) High resolution chiral separation using microfluidics-based membrane chromatography. *J. Chrom. A*, 942: 115–122.
12. Eckelt, J., Loske, S., Goncalves, M.C., and Wolf, B.A. (2003) Formation of micro- and nano-spheric particles (filter dust) during the preparation of cellulose acetate membranes. *Journal of Membrane Science*, 212: 69–74.
13. Desai, T.A., Hansford, D.J., Leoni, L., Essenpreis, M., and Ferrari, M. (2000) Nanoporous anti-fouling silicon membranes for biosensor applications. *Biosensors and Bioelec.*, 15: 453–462.
14. van Rijn, C.J.M., Veldhuis, G.J., and Kuiper, S. (1998) Nanosieves with microsystem technology for microfiltration applications. *Nanotechnology*, 9: 343–345.

15. Hediger, S., Fontannaz, J., Sayah, A., Hunziker, W., and Gijs, M.A.M. (2000) Biosystem for the culture and characterisation of epithelial cell tissues. *Sensors Actuators B*, 63: 63–73.
16. Hediger, S., Sayah, A., Horisberger, J.D., and Gijs, M.A.M. (2001) Modular microsystem for epithelial cell culture and electrical characterisation. *Biosensors and Bioelec.*, 16: 689–694.
17. Surmeian, M., Slyadnev, M.N., Hisamoto, H., Hibara, A., Uchiyama, K., and Kitamori, T. (2002) Three-layer flow membrane system on a microchip for investigation of molecular transport. *Anal. Chem.*, 74 (9): 2014–2020.
18. Tokeshi, M., Minagawa, T., Uchiyama, K., Hibara, A., Sato, K., Hisamoto, H., and Kitamori, T. (2002) Continuous-flow chemical processing on a microchip by combining microunit operations and a multiphase flow network. *Anal. Chem.*, 74 (7): 1565–1571.
19. Russo, A.P., Martin, D., Shain, W., and Turner, J.N. (2002) Microfluidic separations using spin-on polymer membranes. In *Bioinformatics, Proteomics, and Functional Genomics Conference Proceedings*, AIChE Annual Meeting, AIChE: Indianapolis, IN, November 3–8, 2002, 171–180.
20. Russo, A.P., Retterer, S.T., Spence, A.J., Isaacson, M.H., MacColl, R., and Turner, J.N. (2004) Direct casting of polymer membranes into microfluidic devices. *Separation Science and Technology*, 39: 2515–2530.
21. Pekny, M.R., Greenberg, A.R., Khare, V., Zartman, J., Krantz, W.B., and Todd, P. (2002) Macrovoid pore formation in dry-cast cellulose acetate membranes: buoyancy studies. *Journal of Membrane Science*, 205: 11–21.
22. Gokel, G.W., Leevy, W.M., and Weber, M.E. (2004) Crown ethers: Sensors for ions and molecular scaffolds for materials and biological Models. *Chemical Reviews*, 104: 2723–2750.
23. Green, F.J. (1991) *The Sigma-Aldrich Handbook of Stains, Dyes and Indicators*, 2nd ed.; Aldrich Chemical Company, Inc: Milwaukee, WI.
24. Budavari, S. (1996) *The Merck Index*, Twelfth ed.; Merck & Co., Inc: Whitehouse Station, NJ.
25. Frisch, M.J., Trucks, G.W., Schlegel, H.B., Scuseria, G.E., Robb, M.A., Cheeseman, J.R., Zakrzewski, V.G., Montgomery, J.A., Stratmann, R.E., Burant, J.C., Dapprich, S., Millam, J.M., Daniels, A.D., Kudin, K.N., Strain, M.C., Farkas, O., Tomasi, J., Barone, V., Cossi, M., Cammi, R., Mennucci, B., Pomelli, C., Adamo, C., Clifford, S., Ochterski, J., Petersson, G.A., Ayala, P.Y., Cui, Q., Morokuma, K., Malick, D.K., Rabuck, A.D., Raghavachari, K., Foresman, J.B., Cioslowski, J., Ortiz, J.V., Stefanov, B.B., Liu, G., Liashenko, A., Piskorz, P., Komaromi, I., Gomperts, R., Martin, R.L., Fox, D.J., Keith, T., Al-Laham, M.A., Peng, C.Y., Nanayakkara, A., Gonzalez, C., Challacombe, M., Gill, P.M.W., Johnson, B.G., Chen, W., Wong, M.W., Andres, J.L., Head-Gordon, M., Replogle, E.S., and Pople, J.A. (1998) *Gaussian 98* (Revision A1); Gaussian Inc.
26. Mohamed, H., Szarowski, D.H., Lepak, L.A., Spencer, M.G., Martin, D.L., Caggana, M., and Turner, J.N. (2005) Purification of PCR-inhibitory components by cellulose acetate membranes, *Proceedings of the 2005 NSTI Bio Nano Conference*, Vol. 1, 446–448.
27. Mohamed, H., Russo, A.P., Szarowski, D.H., McDonnell, E., Lepak, L.A., Spencer, M.G., Martin, D.L., Caggana, M., and Turner, J.N. (2006) Development and characterization of on-chip biopolymer membranes. *J. Chromatogr. A*, 1111: 214–219.